JOURNAL OF GEOPHYSICAL RESEARCH, VOL. 93, NO. C7, PAGES 8215–8220, JULY 15, 1988

Measurements of the Angle Between the Wind Vector and Wind Stress Vector in the Surface Layer Over the North Sea

G. L. GEERNAERT

Navy Center for Space Technology, Naval Research Laboratory, Washington, D. C.

Measurements of surface layer turbulence, in addition to full meteorological and oceanography quantities, over the North Sea indicated that the stress vector on long time scales is often aligned with a direction slightly different from the mean wind flow. When stratifications were near neutral, the angle difference between the stress and wind exhibited a dependence on the heat and momentum fluxes. In general, the stress vector was observed to be to the left of the flow during stable stratifications, while for unstable stratifications, it was to the right. This finding was consistent using two independent sets of wind stress data, i.e., from MARSEN (1979) and the North Sea Platform Winter Exercise (1985).

1. INTRODUCTION

The magnitude and direction of the wind stress exerted on the ocean surface have a direct impact on a multitude of physical processes. The downward momentum flux (or wind stress) enters the sea surface generating waves, a surface current, and turbulence on both sides of the interface. Boundary layer depth, flux spectra, diffusion rates, surface roughness, and entrainment similarly require information on the surface stress. The air-sea environment is complicated in that the mean and fluctuating flows on both sides of the interface are dependent not only on one another but also on the nature of the interface.

The wind stress τ exerted on the ocean surface is commonly determined by applying the bulk aerodynamic method, such that the stress magnitude is proportional to the square of the wind speed U, i.e.,

$$|\tau/\rho| = C_D U^2 \tag{1}$$

where ρ is the air density. The coefficient of proportionality, (i.e., the drag coefficient C_D) is a function of the measurement height z, roughness length z_0, and stratification ψ, i.e.,

$$C_D = F(z, z_0, \psi) \tag{2}$$

Typically, the roughness length is related to the sea state (see, for example, *Geernaert et al.* [1986]), ψ is scaled via diabatic profile relations [see *Businger et al.*, 1971], and a standard magnitude for z of 10 m is chosen for modelers and experimentalists alike. The direction of the stress vector is typically assumed to be aligned with the wind, and one may also find the bulk parameterization for wind drag written in a vector form similar to

$$\boldsymbol{\tau} = \rho C_D \mathbf{U}_{10}|\mathbf{U}_{10}| \tag{3}$$

See, for example, *O'Brien et al.* [1977] and *Haltiner and Williams* [1980].

Even though the stress vector via the eddy-correlation technique is properly written as

$$\tau/\rho = -\langle u'w'\rangle i - \langle v'w'\rangle j \tag{4}$$

where u', v', and w', are the fluctuating longitudinal, lateral, and vertical velocities, respectively, and i and j are unit vectors aligned with the U and V components, many investigators [e.g., *Geernaert et al.*, 1986; *Busch*, 1977; *Large and Pond*, 1981] incorrectly defined the eddy-correlation stress by either ignoring the $\langle v'w'\rangle$ term or by assuming that it is either unimportant or insignificant with respect to the $\langle u'w'\rangle$ term. If the $\langle v'w'\rangle$ is in fact unimportant, it is by implication that the stress and wind vectors are aligned in the same direction. Generalizing the problem, we define here an angle θ such that

$$\tan\theta = \langle v'w'\rangle/\langle u'w'\rangle \tag{5}$$

where positive angles correspond to the stress vector oriented to the right of the wind vector.

As long as conditions remain reasonably steady and horizontally homogeneous, both the stress magnitude and direction have been assumed to be relatively constant in the lowest 10% of the planetary boundary layer, i.e., within the so-called surface layer [*Panofsky and Dutton*, 1984; *Busch*, 1977]. Recent studies [e.g., *Joffre*, 1985] have shown that in the case of a rapid change in wind speed or direction the surface layer can exhibit a profile of the wind stress magnitude that can largely complicate the nature of the surface layer turbulence structure. With the exception of *Smith* [1980] and *Zemba and Friehe* [1987] there has been a general lack of investigation concerning the angle between the stress and wind vectors, either theoretically or experimentally.

In order to examine the change in the direction between the stress and wind vectors with height, whether for steady or rapidly changing conditions, we may employ the Navier-Stokes equations in the form

$$\frac{dU}{dt} = f(V - V_g) - \frac{\partial}{\partial z}\langle u'w'\rangle \tag{6}$$

$$\frac{dV}{dt} = -f(U - U_g) - \frac{\partial}{\partial z}\langle v'w'\rangle \tag{7}$$

where U and V represent longitudinal and lateral wind speed components in the reference frame of the surface layer flow, and the subscript g indicates geostrophic components. If there exists large-scale warm or cold air advection, (6) and (7) must be coupled with the thermal wind relationship, i.e.,

$$(\partial U_g/\partial_z, \partial V_g/\partial z) = g/fT\,(-\partial T/\partial y, \partial T/\partial x) \tag{8}$$

For the moment, we will assume that regardless of the stratification, thermal advection is insignificant and utilize the Navier-Stokes equation to infer a dependence of the angle θ on the stratification and wind speed.

Paper number 8C0271.

Defining the wind speed profile in the form

$$U = (u^*/k)(\ln (z/z_0) - \psi) \qquad (9)$$

where the friction velocity u^* is $|\tau/\rho|^{1/2}$, equations (9) and (7) may be combined; integrating between z_0 and z results in

$$\langle v'w' \rangle = -\frac{zfu^*}{k}(kC_D^{-1/2} - 1) + fU_g z + \frac{fu^*}{k}\int_{z_0}^{z} \psi \, dz \qquad (10)$$

If stratifications are near neutral, we can for simplicity define the function ψ as $-\beta(z/L)$, where L is the Monin-Obukhov length [after *Businger et al.*, 1971]. We will note that β has values in the neighborhood of 5 for stable stratifications and much smaller values, i.e., of the order of 2, for unstable flows. The Monin-Obukhov length is related to the wind stress and heat flux $\langle w'T_v' \rangle$ according to

$$L = T_a u^{*3}/(gk\langle w'T_v' \rangle) \qquad (11)$$

where T_a is the air temperature, T_v' is the fluctuating virtual temperature, g is gravity, and k is the von Karman constant (=0.4).

Normalizing (9) by the quantity $(-u^{*2})$ and combining with (5), we obtain

$$\tan \theta = (fz/ku^*)(kC_D^{-1/2} - 1 - kU_g/u^*) + (\beta/2k)(zf/u^*)(z/L) \qquad (12)$$

Considering typical surface layer values of $u^* = 0.3$ m/s, $z = 10$ m, $C_D = 0.0012$, $U_g = 12$ m/s, $k = 0.4$, and $f = 10^{-4}$ s^{-1}, the first term on the right-handside of (12) produces absolute values (in degrees) of the order of 2°. The second term on the right-handside, due to the diabatic wind profile, will produce even smaller values: if z/L is -0.2, we calculate 0.1°, while for $z/L = 0.2$, we get -0.2°. With this sample calculation one could easily conclude that for all practical purposes, there is no difference between the directions of the wind and wind stress vectors.

Recent aircraft measurements collected over the oceans by *Zemba and Friehe* [1987] showed that at levels well within the "classical" surface layer (i.e., heights less than a tenth of the PBL depth), angles between the stress and wind vectors were at least an order of magnitude larger than the predictions using the Navier-Stokes equations. Their data suggested a strong dependence on height (with the two vectors aligned at the surface), and magnitudes of the angle often exceeded 90° in the upper reaches of the surface layer. Since Zemba and Friehe's data were collected in the coastal region off California (during CODE), the presence of the coastal jet was attributed to causing, at least in large part, the large magnitudes of the angle θ. If the Navier-Stokes equations are reanalyzed by including the acceleration terms, the estimated departure of the stress vector direction from the wind direction is again much less than the large differences observed in the surface layer over the California current.

In this paper, we will present wind stress vector measurements collected over the North Sea from two sites, where our findings similarly found significant nonzero angles between the stress and wind. In section 2 we present the measurement program and two independent data sets collected from stable platforms, where the measured angle between the stress and wind vectors were presented in terms of stratification. In section 3 we present arguments from a cospectral eddy-flux point of view which serve to suggest a possible mechanism for these large angles, while in section 4, a special case containing periodicities in the angle θ is described in terms of inertial oscillations. Finally, we will summarize in section 5 the implication of these results in remote sensing and air-sea modeling.

2. Data Sets

Two North Sea data sets were analyzed and compiled to investigate the nature of the angle θ. The first is based on measurements of the wind stress with a Gill Propeller Vane Anemometer over the North Sea from a needle (i.e., PISA NEEDLE) planted in the North Sea prior to the MARSEN experiment. The second data set is based on stress measurements using a sonic anemometer mounted on a boom extending west of the North Sea Platform (FPN). Both the Gill and sonic anemometers are capable of sampling at a high frequency the three components of wind speed fluctuations, thereby producing measurements of the stress components $\langle v'w' \rangle$ and $\langle u'w' \rangle$. The averaging time chosen for the covariance calculations depends on measurement height; typically, 30 min was chosen; for the extremely high wind speeds, we used 10 min. Both the Pisa and FPN data sets have previously been analyzed but only in terms of the drag coefficient dependence on sea state; see *Geernaert et al.* [1986] and *Geernaert et al.* [1987], respectively, for details.

Since our examination here concerns small angular deviations from the mean flow, an obvious concern is data quality with respect to platform flow distortion. The PISA data set was collected 2 m to the west of a vertical mast of 40 cm diameter, where the system was mounted on a cross-arm 7.5 m above the mean sea level. The local water depth at Pisa was approximately 15 m. Because the surface area exposed to the flow at Pisa was both small and significantly downwind of the measurement site, it was concluded by *Geernaert et al.* [1986] that the data exhibited no significant influence of the platform for three of the four wind azimuth quadrants. Data from the North Sea Platform (FPN) were collected from a boom extending 20 m to the west and 7 m above the body of the platform. The area exposed to the flow by FPN is 26 m × 10 m. For the relative location of the sonic anemometer a laboratory simulation of flow distortion around the FPN indicated that insignificant distortion of the wind vector by the structure would be expected if southwesterly through northwesterly winds were considered. For both data sets the sensors were mounted on the west side of the respective platforms, and the subsequent wind and wave fields were characteristic of long upwind fetch. The FPN data set considered for this analysis therefore includes wind vectors with azimuths between 220° and 300°. The Pisa data set included wind vectors from the entire western hemisphere of azimuths. For our initial analysis we required that the calculated 10-m-height wind speed was greater than 10 m/s in order to assure that the data from both Pisa and FPN were well within the surface layer. Both data sets were representative of open ocean conditions since upwind fetches were at a minimum 200 km.

Due to the higher wind speeds reported in this study, calculations of the Monin-Obukhov length were generally such that $|L| > 100$ m; that is, large departures of the stratification from neutral were preferentially eliminated from the data set. The calculation of L was based on measured heat fluxes during the FPN exercise and use of the bulk method during the Pisa measurement program; for more details, the reader is referred to *Geernaert et al.* [1986, 1987].

For this study the data from each experiment were, at first, analyzed independently; the data analysis was subsequently performed on the compilation of both data sets. Based on an initial inspection, the angle θ appeared to have a larger variability within the North Sea Platform data, where the measurement height was 33 m, when compared to Pisa, where the height was 7 m. For both data sets, unstable stratifications seemed to correspond to positive angles, while stable stratifications were associated with negative angles. In contrast to poor results we obtained when θ was plotted against z/L (see Figures 1 and 2), a high correlation was found between θ and the quantity $U(T_0 - T_{10})$, where subscripts indicate the measurement height above the surface; see Figures 3 and 4. The best fit linear regression equations were found to be

$$\theta_{\mathrm{PISA}}° = 0.12U(T_0 - T) - 0.3° \qquad \pm 4.7° \qquad (13)$$

$$\theta_{\mathrm{FPN}}° = 0.53U(T_0 - T) - 4.2° \qquad \pm 12° \qquad (14)$$

where the correlation coefficients were found to be 0.61 and 0.62 for FPN and PISA, respectively, and all units are MKS. It is noteworthy to point out that while the ratio of the measurement heights between FPN and Pisa was approximately 5, the ratio of the regression line was similarly found to be about 5. Letting the angle θ depend linearly on height and noting that the heat flux $\langle w'T' \rangle$ may be written in a bulk form according to

$$\langle w'T' \rangle = C_H U_{10}(T_0 - T_{10}) \qquad (15)$$

equations (13)–(15) may be combined to yield a best fit relation using both data sets to yield

$$\theta° = 15.4z\langle w'T' \rangle - 0.83° \qquad \pm 6.6° \qquad (16)$$

As in (13) and (14), the units in (15) are MKS, and a correlation coefficient of 0.58 is obtained. For both the Pisa and FPN data sets, values of C_H were chosen for stable and unstable stratifications to be 0.86×10^{-3} and 1.08×10^{-3}, respectively [*Smith*, 1980]. See Figure 5. Equation (16) implies a first-order estimate of the heat flux and the stratification to be

$$\langle w'T' \rangle = 0.06z^{-1}\theta° \qquad (17)$$

and

$$z/L = 0.60°/U^3 \qquad (18)$$

where $z \gg 0$ while one remains within the surface layer. Equation (18) is based on, for illustration only, a C_D of 1.2×10^{-3}; $T = 290$°K; $k = 0.4$; and again all units are MKS, while θ is in degrees. At this point, we must be reminded that more data must be both collected and analyzed before (16)–(18) can be applied to the oceanic environment.

Equations (13)–(18) have a physical drawback in that a statistical relationship has been drawn with quantities that have not been normalized or nondimensionalized. Stepping back to the Navier-Stokes equation, we found that the stratification contribution to the angle θ scaled with the quantity $(zf/u^*)(z/L)$; using 7 and 33 m, a linear fit produces, for each

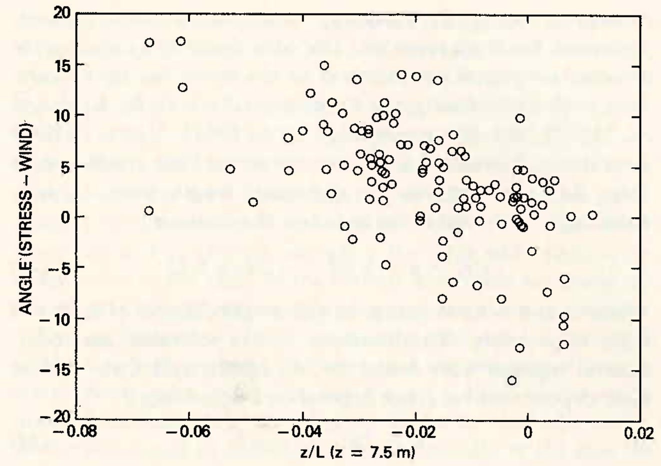

Fig. 1. Distribution of the angle between the stress and the wind as a function of z/L at Pisa where $z = 7.5$ m.

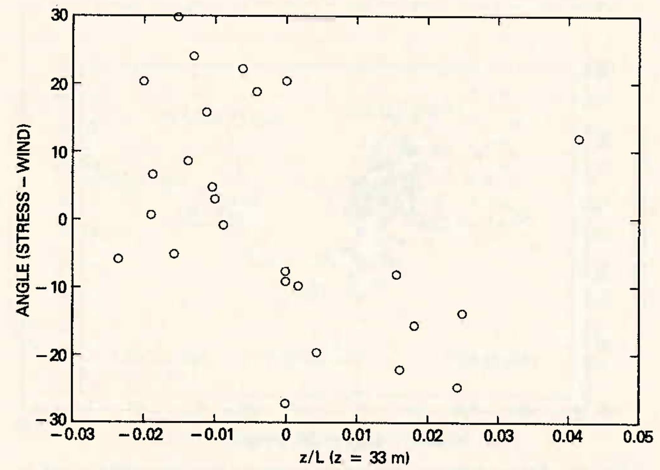

Fig. 2. Distribution of the angle between the stress and the wind as a function of z/L at FPN where $z = 33$ m.

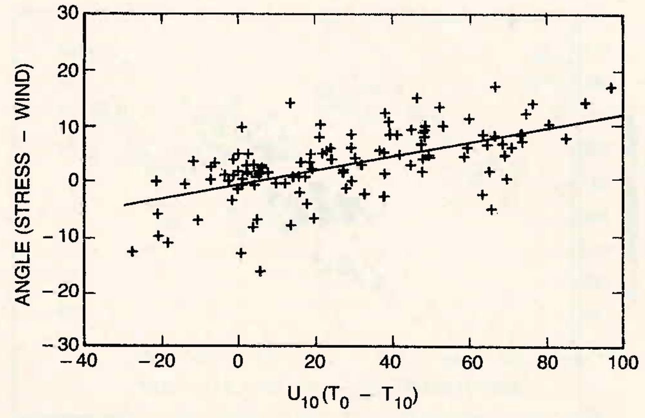

Fig. 3. Influence of heat flux on the MARSEN wind stress vector direction using data collected on the PISA needle at 7.5 m elevation. Only wind speeds greater than 10 m/s from the western azimuth hemisphere are included.

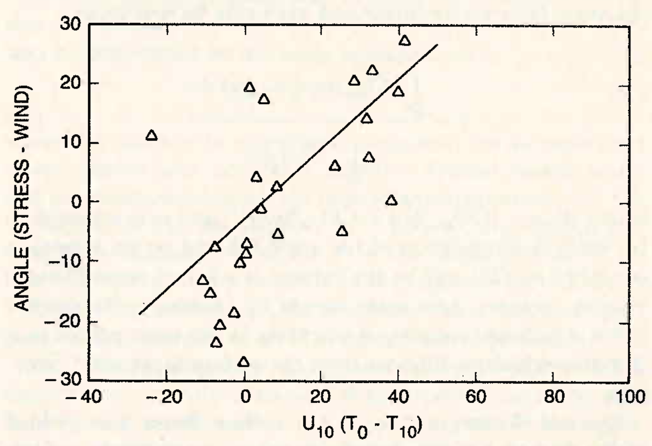

Fig. 4. Influence of heat flux on the North Sea Platform wind stress vector direction using data collected at 33 m height. Only 10 m/s or greater winds from southwest through northwest are included.

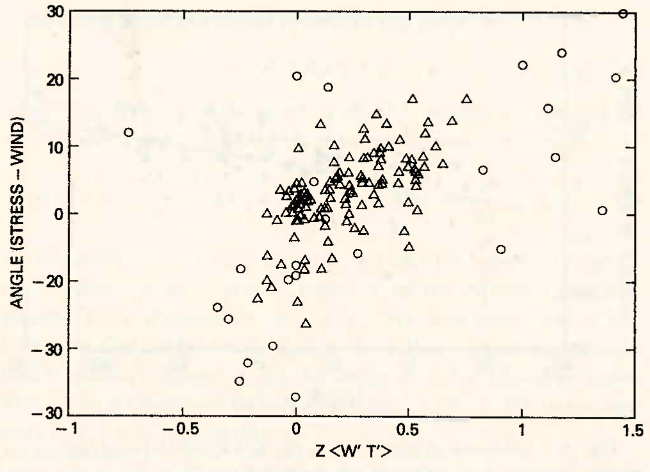

Fig. 5. Dependence of the angle between the stress and the wind on the calculated heat flux (using both data sets). Triangles are PISA data, while circles are FPN data.

data set, the following relations:

$$\theta_{\mathrm{PISA}}{}^\circ = K_P(zf/u^*)(z/L) + 0.47^\circ \qquad \pm 5.3^\circ \tag{19}$$

$$\theta_{\mathrm{FPN}}{}^\circ = K_F(zf/u^*)(z/L) + 0.89^\circ \qquad \pm 14.8^\circ \tag{20}$$

where K_P and K_F were determined to have best fit values of -9.3×10^4 and -6.3×10^4, respectively. Correlation coefficients for the PISA and FPN data sets were determined to be -0.48 and -0.39, respectively. Combining the two data sets, the best fit relation now becomes (see Figure 6)

$$\theta^\circ = K_C(zf/u^*)(z/L) + 0.31^\circ \qquad \pm 6.1^\circ \tag{21}$$

with a correlation coefficient of -0.31, and a value for K_C of -1.0×10^5. We note here that the angle between the stress and wind exhibits a better linear fit with the heat flux than with the nondimensional relation $(zf/u^*)(z/L)$. A clear difference between (16) and (21) is that the former depends linearly on height, while the latter scales with the square of the measurement height.

3. DISCUSSION

In order to understand why the predictions of the angle using the Navier-Stokes equations (equation (12)) were significantly smaller than the magnitudes obtained from both the North Sea data sets and the measurements of Zemba and Friehe, we suggest a cospectral eddy-flux viewpoint, such that the angle between the stress and wind may be written as

$$\theta = \frac{\int_0^\infty \mathrm{Co}_{vw}(\omega)/\mathrm{Co}_{uw}(\omega)\, d\omega}{\int_0^\infty A(\omega)\, d\omega} \tag{22}$$

where $A(\omega) = \{\mathrm{CO}_{uw}{}^2(\omega) + \mathrm{CO}_{vw}{}^2(\omega)\}^{1/2}$ and ω is assumed to be small. A formulation of the angle θ based on an approach described by (22) will be the subject of a future investigation; we can, however, gain some insight by examining the mechanisms which are capable of orienting larger-scale eddies in a direction which is different from the surface layer wind direction.

Spectral decomposition of the surface fluxes has yielded scale relations that are based on measurement height z, sampling frequency, and stratification (in terms of z/L). With the large scatter in the compiled flux cospectra data sets [e.g., *Kaimal et al.*, 1972; *Caughey*, 1982], no concrete parameterization has been reported. The eddy frequency carrying the greatest cospectral contribution to the stress has been examined both theoretically and experimentally both by *Kaimal et al.* [1972] and *Wyngaard and Cote* [1972]. Using Taylor's hypothesis, Wyngaard and Cote converted their results into a form that characterizes the dominant length scale λ_0, contributing to the total stress to follow the relation

$$z/\lambda_0 = a + b\, z/L \qquad z/L > 0.25 \tag{23}$$

where a and b have values in the neighborhood of 0.25 and 0.30, respectively. Stratifications in the unstable and near-neutral regimes were found by Wyngaard and Cote to lose their dependence on L but depend on z according to

$$\lambda_0 = 10z \qquad L < 0 \tag{24}$$

At this point, we assume for simplicity that large eddies are circular (even though they are most likely oblate) and define λ_0 as an eddy height scale as well as a horizontal length scale. It is noteworthy to point out that the real height scale is most likely smaller than λ_0. Noting here that the boundary layer over the ocean has a depth which can to first-order and near-neutral stratifications be approximated as ku^*/f [*Tennekes*, 1982], the height of the surface layer, h, will be $ku^*/10f$. With this, the dominant eddy will be above the surface layer for unstable flow if the sampling height z is greater than $ku^*/100f$. For the Pisa and FPN data sets this roughly corresponds to $U < 6.5$ m/s and $U < 28$ m/s, respectively.

For stable flow the condition for $\lambda_0 > h$ becomes

$$z > aku^{*3}T_a/[10T_a fu^{*2} + bgk^2\langle w'T'\rangle/T_a] \tag{25}$$

If the wind speed is 10 m/s, (24), implies that $(T_a - T_0)$ must be less than 1°C for the Pisa data; for the FPN data set, significantly higher wind speeds and air-sea temperature differences must be observed for the dominant eddy scale to exceed the surface layer depth. For both stable and unstable stratifications the scale length λ_0 is assumed to represent only the dominant eddy of the momentum flux cospectrum; there are, however, a full myriad of eddies with scales both longer and shorter than λ_0 which contribute to the total stress.

Given that larger-scale eddies within the mixed layer (above the surface layer) provide important contributions to the total surface momentum flux, it follows that the vector orientation of these large eddies with respect to the surface layer flow may

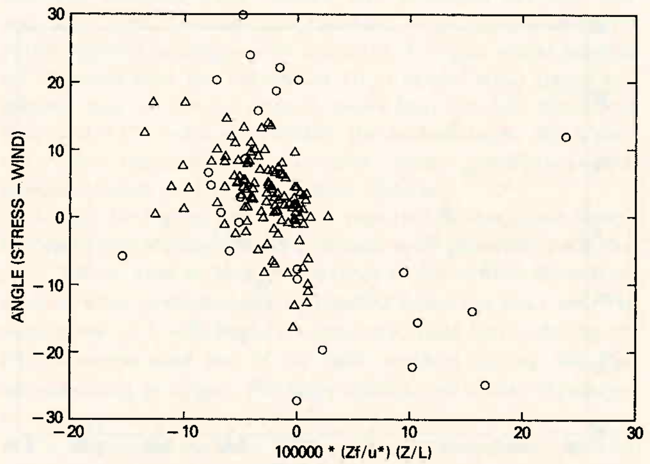

Fig. 6. Dependence of the angle between the stress and wind on the quantity $(zf/u^*)(z/L)$ using both FPN and PISA data. Triangles represent Pisa data, while FPN data are represented by circles.

play a role in the angle in which they transmit momentum downward (with respect to the surface layer wind direction). Clearly, warm air-advection is associated with a rotation of the wind vector to the left with height, while cold air advection turns the wind flow to the right. It immediately follows that eddies generated by perturbations along the inversion or upper boundary layer shear instabilities will have vector propagation directions which may differ from the surface layer wind vector. For cold air advection the large eddy vectors are likely to be to the right of the surface flow while for warm air advection the large eddy vectors are oriented more to the left.

During December 1985 a continuous time series of data was collected which spanned 18 hours and the passage of both a warm front and a cold front. See Figure 7. Prior to the warm front, stratifications were slightly unstable, and the stress vector was found to consistently be to the right of the flow (in the surface layer at 33 m elevation). After passage of the warm front the surface layer became stably stratified with warm air advection; the stress vector in this case was found to consistently be to the left of the surface layer flow. At approximately 0300 on December 6, 1985, the cold front passed the North Sea Platform (FPN), and cold air advection with unstable stratifications immediately prevailed; the stress vector within the cold sector was found to be consistently to the right of the wind flow.

The orientation of eddies within the boundary layer are not only linked to the magnitude and orientation of the thermal wind vector but also to the physical mechanisms which generated the large eddies. Little is known about eddy generation mechanisms, but it is presumed that perturbations at the top of the PBL near the inversion are equally as important as shear and buoyancy instabilities within the boundary layer. The proportion of eddies of all scales that are governed by perturbations near the inversion would be useful toward a future variational analysis of the angle between the stress and wind. These questions are currently unresolved and are expected to be important in describing the momentum flux cospectrum in the surface layer.

4. INERTIAL OSCILLATIONS

While we have thus far restricted our analysis to moderate to high wind speeds, an interesting observation of the angle θ was noted in the case of stable flow and light to moderate southwest winds. See Figure 8. Starting on December 4, 1985, these data represent southwesterly wind azimuths, wind speeds in the neighborhood of 7–9 m/s, air-sea temperature

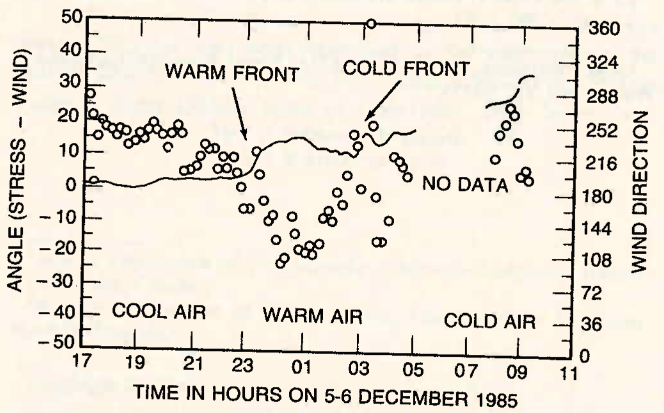

Fig. 7. Time series of the angle between the stress and wind during the passage of an intense North Sea storm on December 5–6, 1985 (circles), and wind azimuth (solid curve).

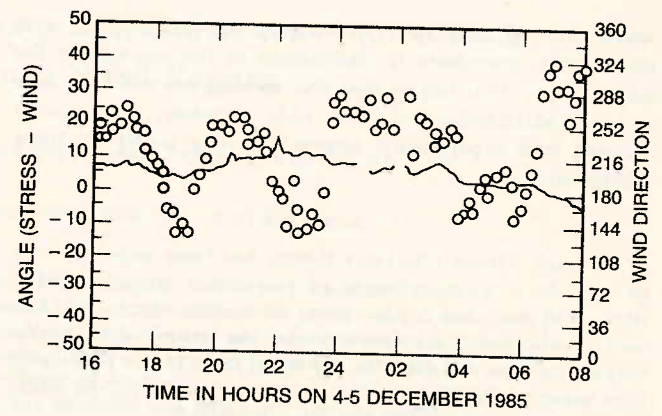

Fig. 8. Time series of the angle between the stress and wind during for stable flow and moderate wind speeds over the North Sea (circles) and wind azimuth (solid curve).

differences of the order of 2°C, and averaging times of 10 min for each record. On first inspection, it appeared that the angle was periodic on a time scale of 3–4 hours. The measurement height for these data was 33 m. Pressure maps indicated that during this period, light winds prevailed over the North Sea, and the barometer record on the North Sea Platform showed a decreasing atmospheric surface pressure. While the records showed a significant periodicity in the angle between the stress and wind, the wind vector direction exhibited very little periodicity.

To try and explain this phenomenon, one may resurrect the Navier-Stokes equations by retaining the acceleration terms and assume that since the flow is stable with light wind speeds, the stress terms can, at first, be neglected. Equations (6) and (7) may now be written as

$$d(U - U_g)/dt = f(V - V_g) \tag{26}$$

$$d(V - V_g)/dt = -f(U - U_g) \tag{27}$$

where we assume that $dU_g/dt = dV_g/dt = 0$. Differentiating (26) and (27) and combining, one easily obtains a periodic solution of the form

$$(U - U_g, V - V_g) = (U_0, V_0) \sin ft \tag{28}$$

where U_0 and V_0 are mean states and U and V become periodic with a time scale of $2\pi/f$, i.e., the inertial time scale. It is important, however, to point out that this time scale is with respect to the moving air mass. Taking into account advection, the time scale T with respect to a point on the surface may be determined by including advection, i.e.,

$$2\pi/T = f + (KU)_{\mathrm{am}} \tag{29}$$

where the quantity in parentheses represents the air mass (am) wave number and advection velocity. Typical length scales and propagation velocities for mesoscale disturbances over the wintertime North Sea are 10^{-5} m^{-1} and 20 m/s, respectively, thereby producing a value for T in the neighborhood of 4.6 hours, which is slightly larger than the observed periodicity in Figure 8; uncertainty in the advection rates, however, produces a large margin for error in the calculated periodicity.

The actual mechanisms that govern such periodicities in the angle θ are currently unknown. It is suspected here that perhaps inertial oscillations in the wind field exist in the upper reaches of the planetary boundary layer (PBL). If oscillations in these upper levels do exist while the wind flow in the lower part of the stable PBL does not exhibit such oscillations, the vector flux of momentum carried by the large upper level eddies may contribute to oscillations in the angle θ in the surface layer. It is hoped that this speculation will lead to a deeper understanding of PBL eddy dynamics and spectra through field experiments, especially during stably stratified conditions.

5. SUMMARY

Although Monin-Obukhov theory has been widely shown to provide a good estimate of turbulence structure, wind stress, and heat flux for a variety of stratifications, little has been mentioned in the literature on the nature of the stress vector direction relatively to the mean flow. It has previously been assumed that at least within the surface layer, the stress and wind are identically in the same direction.

Data from two North Sea experiments were reanalyzed to examine the dependence of the stress vector direction on the atmospheric stratification. In general, it was found that for unstable flow the stress vector was slightly to the right of the local wind. For the stable case the vector was found to be to the left of the flow. We found one case representative of stable stratifications where the sign of the angle between the stress and the wind exhibited a periodicity of the order of 3–4 hours; this periodicity was argued to be due to inertial oscillations within a boundary layer air mass which was advecting past the measurement site.

These results pose new questions on several facets of marine boundary layer research and ocean surface remote sensing experiments. The systematic variations in the stress in the region of storms suggest that there exists a convergence of downward turbulent momentum flux near cold fronts and a divergence near warm fronts. Similarly, the vertical structure of the divergence and convergence pattern about the front may differ, depending upon whether the front is cold or warm; this issue cannot easily be addressed with the data presented herein.

For the sampling of wind stress via low flying aircraft as part of large-scale remote sensing calibration/validation campaigns, a new issue is raised here: Is the wind stress vector measured at aircraft level comparable to the real stress exerted near the air-sea interface? It is suggested that caution be placed on the interpretation of such data, particularly when there exists a large departure of the thermal stratification from the neutral state.

Since stress data via aircraft also serve to infer calculations of the stress curl, as was determined for FASINEX investigations, errors may evolve solely due to the assumption that the stress and wind uniformly have the same direction throughout the depth of the surface layer. This paper serves to show that, in general, the stress and wind vectors are rarely aligned.

Acknowledgments. The author wishes to acknowledge many useful discussions with Soren Larsen and Torben Mikkelsen of Riso National Laboratory (Roskilde, Denmark), Kristina Katsaros and Bob Brown of the University of Washington, Gene Takle of Iowa State, and Bill Plant of the Naval Research Laboratory. Particular credit is due to helpful comments and discussions with Joost Businger and Erik Mollo-Christensen. This research was supported by the Basic Research Program of the Naval Research Laboratory.

REFERENCES

Busch, N. E., Fluxes in the surface boundary layer over the sea, in *Modelling and Prediction of the Upper Layers of the Ocean*, edited by E. Kraus, pp. 72–91, Pergamon, Elmsford, N. Y., 1977.

Businger, J. A., J. C. Wyngaard, and Y. Izumi, Flux profile relationships in the atmospheric surface layer, *J. Atmos. Sci.*, *28*, 181–189, 1971.

Caughey, S. J., Observed characteristics of the atmospheric boundary layer, in *Atmospheric Turbulence and Air Pollution Modelling*, edited by F. T. M. Nieuwstadt and H. Van Dop, pp. 107–158, D. Reidel, Hingham, Mass., 1982.

Geernaert, G. L., K. B. Katsaros, and K. Richter, Variation of the drag coefficient and its dependence on sea state, *J. Geophys. Res.*, *91*, 7667–7679, 1986.

Geernaert, G. L., S. Larsen, and F. Hansen, Measurements of the wind stress, heat flux, and turbulence intensity during storm conditions over the North Sea, *J. Geophys. Res.*, *92*, 13,127–13,139, 1987.

Haltiner, G. J., and R. T. Williams, *Numerical Prediction and Dynamic Meteorology*, 2nd ed., 477 pp., John Wiley, New York, 1980.

Joffre, S. M., The structure of the marine atmospheric boundary layer: A review from the point of view of diffusivity, transport, and deposition processes, *Tech. Rep. 29*, Finn. Met. Inst., Helsinki, Finland, 1985.

Kaimal, J. C., J. C. Wyngaard, Y. Izumi, and O. R. Cote, Spectral characteristics of turbulence, *Q. J. R. Meteorol. Soc.*, *98*, 563–589, 1972.

Large, W J., and S. Pond, Open ocean momentum flux measurements during moderate to strong winds, *J. Phys. Oceanogr.*, *12*, 464–482, 1981.

O'Brien, J. J., R. M. Clancy, A. J. Clarke, M. Crepon, R. Elsberry, T. Gammelsrod, M. MacVean, L. P. Roed, and J. D. Thompson, Upwelling in the ocean: Two-and three-dimensional models of upper ocean dynamics and variability, in *Modelling and Prediction of the Upper Layers of the Ocean*, edited by E. B. Kraus, pp. 178–228, Pergamon, Elmsford, N. Y., 1977.

Panofsky, H. A., and J. A. Dutton, *Atmospheric Turbulence*, 397 pp., Academic, San Diego, Calif., 1984.

Smith, S. D., Wind stress and heat flux over the oceans in gale force winds, *J. Phys. Oceanogr.*, *10*, 709–726, 1980.

Tennekes, H., Similarity relations, scaling laws and spectral dynamics, in *Atmospheric Turbulence and Air Pollution Modelling*, edited by F. T. M. Nieuwstadt and H. Van Dop, pp. 37–68, D. Reidel, Hingham, Mass., 1982.

Wyngaard, J. C., and O. R. Cote, Cospectral similarity in the atmospheric surface layer, *Q. J. R Meterol. Soc.*, *98*, 590–603, 1972.

Zemba, J., and C. A. Friehe, The marine atmospheric boundary layer jet in the Coastal Ocean Dynamics Experiment, *J. Geophys. Res.*, *92*, 1489–1496, 1987.

G. L. Geernaert, NCST Code 8314, Naval Research Laboratory, Washington, DC 20375.

(Received December 7, 1987;
accepted March 9, 1988.)